ONLINE FIRST January 13, 2026

Engineering Transactions, **74**, https://doi.org/10.24423/engtrans.2025.3453
Institute of Fundamental Technological Research Polish Academy of Sciences (IPPT PAN)
Université de Lorraine • Poznan University of Technology

Research Paper

Multi-Objective Optimization of Hobbing Process Parameters Using the Response Surface Method

Yazhou WANG*, Xiaohui YIN

School of Mechanical and Electrical Engineering,
Lanzhou University of Technology
Lanzhou, China

*Corresponding Author: wangyzh@lut.edu.cn

In hobbing machining, gear geometric accuracy is an important factor affecting gear working performance, and it is determined by the interaction of different process parameters. To improve the geometric accuracy of the hobbing surface and obtain the minimum geometric error, this research adopts the response surface method (RSM) to study the effects of various technological parameters on the geometric accuracy and explores the influence of each factor on the geometric accuracy through the response surface diagram. Mathematical models of total profile deviation, total helix deviation, cumulative total deviation of tooth spacing, and radial runout are established using the RSM, and their reliability is tested by an analysis of variance (ANOVA). A non-dominated sorting whale optimization algorithm (NSWOA) is used to solve the mathematical model, and a Pareto solution set is obtained. The entropy weight-technique for order preference by similarity to the ideal solution (TOPSIS) method is then used to determine the optimal scheme after the NSWOA algorithm optimization. After optimization, the total deviation of tooth profile was reduced by 8.04 %, the total helix deviation was reduced by 9.17 %, the cumulative total deviation of tooth spacing was reduced by 3.88 %, and the radial runout was reduced by 7.45 %, which proves that the optimized scheme can improve the gear accuracy after hobbing machining and it provides a reference for the reasonable selection of gear hobbing process parameters.

Keywords: hobbing machining, response surface method, multi-objective optimization, geometric accuracy.

1. Introduction

Gears are key components that affect the performance of machinery and equipment, and under economic and environmental constraints, industrial practices have increasingly pursued high-precision gear manufacturing technology [1]. Hobbing technology is dominant in the field of gear manufacturing due to its

excellent processing efficiency and extensive process adaptability. Therefore, it is of great significance to study hobbing accuracy to improve the efficiency of gear machining. Sun *et al.* [2] proposed a prediction model for geometric deviation in hobbing and an optimization model for the hobbing process, both of which improved the machining accuracy of hobbing. Hu *et al.* [3] proposed an analytical method for evaluating the hobbing accuracy of flexible spline tooth profiles, which provides a valuable technical reference for error tracking and compensation in the process of hobbing. Wang *et al.* [4] considered energy consumption and gear geometrical deviations to optimize hobbing parameters. Matsuo *et al.* [5] described a hobbing simulation that was considered the first step in improving hobbing accuracy. Their simulation aimed to elucidate the effect of the positional relationship between the workpiece and the tool on gear accuracy, including the pitch error of the workpiece and tooth runout. In order to improve the geometric accuracy of gear hobbing, many researchers have studied process parameters. Zhou *et al.* [6] analyzed the basic principle of dry cutting technology and explored the effect of variations in processing parameters on the cutting process. Dong *et al.* [7] constructed a three-dimensional finite element simulation model to simulate the complex motion between the hobbing tool and the gear workpiece, and conducted a coupled thermodynamic analysis of the tool and the workpiece during the chip removal process. Klockea *et al.* [8] designed a continuous gear-hobbing simulation method capable of numerically reproducing the cutting process in complex processing environments and predicting the geometric profile and surface features of the workpiece.

Process parameter optimization is a key technology for improving the machining performance of hobbing, the core of which is to realize the coordinated improvement of machining efficiency and precision through parameter optimization. Multi-objective optimizations [9] adopt global optimization strategies, establish comprehensive evaluation systems including key indicators such as processing cost, efficiency, and accuracy, and use an impact analysis method to determine the optimal combination of process parameters, thereby achieving overall optimization of processing performance. Kane *et al.* [10] adopted a mathematical modeling method to construct a univariate optimization model aimed at minimizing the processing cost. In their model, hob speed and feed rate served as key decision variables and the optimal process parameter combination was obtained by solving the objective function. Li *et al.* [11] proposed a multi-objective optimization method for process parameters, which considers the minimum heat accumulation in the spindle of a dry gear hobbing machine, effectively reducing its average temperature. Santanna *et al.* [12] selected tool vibration characteristics as the optimization objective and revealed the internal correlation between hobbing process parameters and tool vibration through experimental research methods. On the premise of maintaining the stability of

the tool system, their optimization method increased the machining efficiency by more than 18 %.

The application of intelligent algorithms to process parameter optimization has become one of the current research hotspots in the fields of engineering and manufacturing. Its core objective lies in efficiently finding optimal process combinations through data-driven and intelligent search strategies to enhance production efficiency, reduce costs, or improve product quality [13]. Sun *et al.* [2] took the minimization of gear geometric error as the target, and combined an improved particle swarm optimization algorithm with a backpropagation (BP) neural network to optimize machining parameters. The optimized hobbing parameters improved geometric accuracy of the gear. Wu *et al.* [14] constructed a multi-parameter collaborative optimization framework focused on improving the processing efficiency and economic performance in response to the demand for improving the efficiency of the gear-hobbing process. The authors used the feed rate and cutting speed as key variables and conducted parameter tuning by integrating intelligent algorithms and data-driven prediction models. Their method promotes energy conservation and consumption reduction in the production process while ensuring processing quality by integrating group-optimization strategies and machine learning techniques.

Current research on hobbing process optimization mainly focuses on multi-objective collaborative optimization of energy consumption, machining time, product quality, and cost. With the development of Industry 4.0 and intelligent manufacturing, the optimization goal for gears, key basic components, has shifted from traditional efficiency and economic indicators toward the precise control of geometric accuracy. Key geometric precision indicators such as total profile deviation, total helix deviation, cumulative total pitch deviation, and radial runout directly affect the transmission performance of gear pairs. Therefore, modern hobbing process optimization needs the establishment of a geometric-precision-oriented model that is considered a core optimization goal, and which enables the collaborative optimization of each key index.

2. Methods

2.1. Test conditions

The KE180 hobbing machine from Kashifuji company is used as the hobbing processing equipment; the on-site hobbing equipment and processing area are shown in Fig. 1, while the gear model and the processed gear are shown in Fig. 2. The basic parameters of the hob and the gear are shown in Table 1 [15]. The material of the gear is 20CrMnTi, which has the characteristics of high hardness, good wear resistance, and good toughness, making it widely used in gear manufacturing. Its mechanical properties are shown in Table 2.

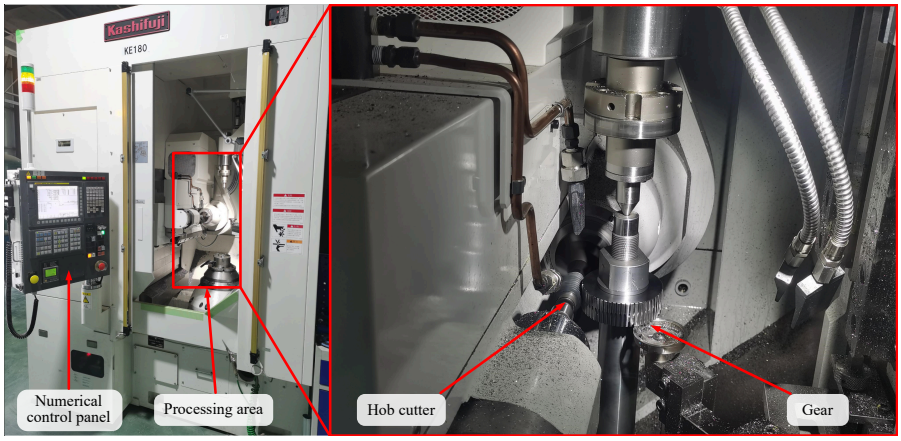

FIG. 1. Hobbing equipment and processing area.

a)

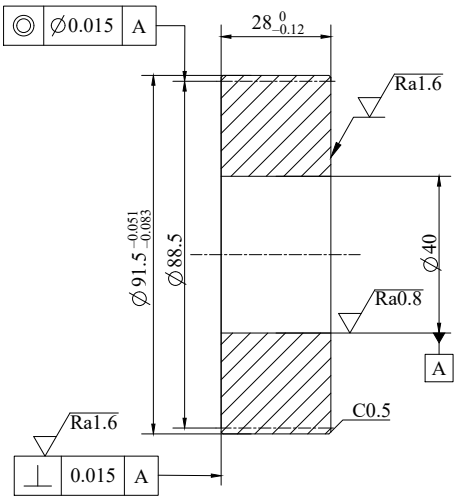

b)

FIG. 2. Gear model (a) and machined gears (b).

TABLE 1. Main parameters of hobs and gears.

Hob parameters		Gear parameters	
Normal modulus [mm]	1.5	Modulus [mm]	1.5
Number of heads	1	Number of teeth	59
Normal pressure angle [°]	20	Pressure angle [°]	20
Spiral rising angle	3°3′	Tooth width [mm]	28

TABLE 2. Mechanical properties of 20CrMnTi.

Tensile strength [MPa]	Yield strength [MPa]	Elongation [%]	Section shrinkage [%]
≥1080	≥835	≥10	≥45

2.2. Test scheme

During the test process, only the machining parameters (hob speed V, feed rate f, and back engagement D) are changed to explore the influence of hobbing process parameters on geometric accuracy. The basic deviations of the gear tooth surface (total deviation of tooth profile F_α, total deviation of helix F_β, cumulative total deviation of tooth spacing F_p, and radial runout F_r) were selected as evaluation indices for geometric accuracy [16, 17]. The difference in back engagement represents the difference in the number of cuts. To facilitate easy operation and software analysis, back engagement D is expressed by the number of cuts D_t. The test scheme for three factors and three levels is obtained, with the test factors and levels listed in Table 3. The Box-Behnken design (BBD) method is used to design the response surface test [18], and Design-Expert software is used to conduct the test design. A total of 17 tests are conducted, and the test scheme is shown in Table 4.

Table 3. Test factors and level.

Level	Hob speed [r/min]	Feed rate [mm/min]	Back engagement [mm] (number of cuts)
1	450	2.0	0.84375 (4 times)
2	600	2.75	1.125 (3 times)
3	750	3.5	1.6875 (2 times)

Table 4. Response surface test scheme.

No.	Hob speed [r/min]	Feed rate [mm/min]	Back engagement [mm]	No.	Hob speed [r/min]	Feed rate [mm/min]	Back engagement [mm]
1	600	2.75	1.125	10	600	2.75	1.125
2	750	2.0	1.125	11	600	2.0	0.84375
3	600	3.5	0.84375	12	600	3.5	1.6875
4	600	2.75	1.125	13	450	2.75	1.6875
5	750	3.5	1.125	14	600	2.75	1.125
6	600	2.0	1.6875	15	450	2.75	0.84375
7	750	2.75	0.84375	16	600	2.75	1.125
8	750	2.75	1.6875	17	450	2.0	1.125
9	450	3.5	1.125	–	–	–	–

2.3. Geometric accuracy measurements

The Japanese OSAKA Precision CLP-35SF automatic gear-measuring instrument is used to measure gear geometric errors, and the on-site measure-

ment equipment and measurement area are shown in Fig. 3 [19]. The testing specification is implemented according to International Organization for Standardization [17], and the detection precision level is determined according to the same standard. As shown in Fig. 4, the total deviation of tooth profile and the total deviation of helix were measured at 8 measurement positions on the left and right tooth surfaces of four gear teeth numbered 01, 16, 31, and 46. The corresponding higher values of the total deviation of tooth profile and total deviation of helix at each position were selected for analysis [16]. The cumulative total deviation of tooth spacing and the radial runout were measured on the left and right flanks of the 59 teeth of each gear, and the average values of the cumulative total deviation of tooth spacing and the radial runout were selected for analysis [20].

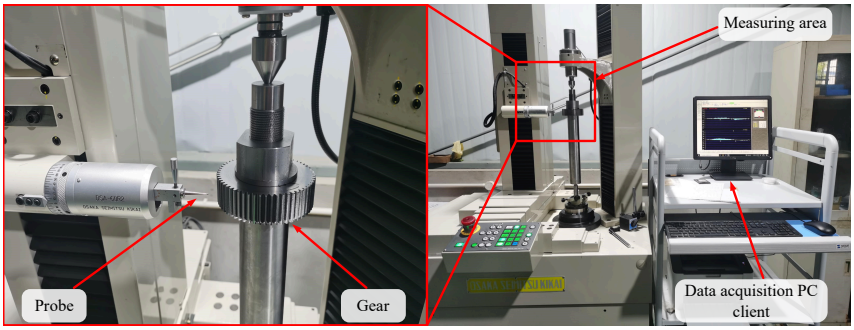

FIG. 3. Measurement process using the CLP-35SF fully automatic gear measuring instrument.

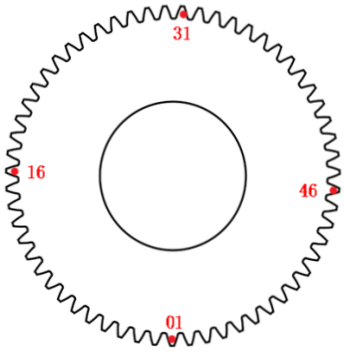

FIG. 4. Schematic diagram of the measurement locations for total profile deviation and total helix deviation.

2.4. Optimization based on non-dominated sorting whale optimization algorithm

Different from the unique optimality of a single-objective function, the multi-objective function model should consider the mutual restriction and influence of

multiple objective functions. In the process of gear hobbing, ensuring the machining geometric accuracy is the primary condition for meeting performance requirements. Total profile deviation, total helix deviation, cumulative total pitch deviation, and radial runout are the key optimization objectives, and their mutual restriction relationship and synergistic influence should be comprehensively considered. Therefore, multi-objective optimization was carried out with the hobbing process parameters (hob speed, feed rate, and back engagement) as optimization variables, and total profile deviation, the total helix deviation, the cumulative total deviation of tooth spacing and the radial runout as the optimization objectives.

2.4.1. Optimization objectives and constraints. The non-dominated sorting whale optimization algorithm (NSWOA) was used to optimize the total profile deviation, the total deviation of helix, the cumulative total deviation of tooth spacing and the radial runout. The difference in back engagement represents the difference in the number of cuts. In order to facilitate calculation, back engagement D is expressed in terms of the number of cuts D_t. Therefore, the NSWOA algorithm is used to optimize and combine V, f, and D_t. Based on the set range of process parameters, the distribution intervals of measurement data, and the minimum characteristic values of the optimization objective, constraint conditions are established. The optimization objectives and constraint conditions are as follows:

$$
\begin{cases}
\min F_\alpha(V, f, D_t), \\
\min F_\beta(V, f, D_t), \\
\min F_p(V, f, D_t), \\
\min F_r(V, f, D_t), \\
9\,\mu\text{m} \le F_\alpha(V, f, D_t) \le 12.8\,\mu\text{m}, \\
22\,\mu\text{m} \le F_\beta(V, f, D_t) \le 47.9\,\mu\text{m}, \\
10.5\,\mu\text{m} \le F_p(V, f, D_t) \le 52.8\,\mu\text{m}, \\
13.2\,\mu\text{m} \le F_r(V, f, D_t) \le 58.8\,\mu\text{m}, \\
450\,\text{r/min} \le V \le 750\,\text{r/min}, \\
2\,\text{mm/min} \le f \le 3.5\,\text{mm/min}, \\
2\text{ times} \le D_t \le 4\text{ times},
\end{cases}
\tag{2.1}
$$

where V, f, and D_t represent hob speed, feed rate, and the number of cuts, respectively.

The penalty function method is adopted to handle the constraint conditions, and the form of the penalty function is as follows:

$$\Phi_k(x) = f_k(x) + P(x), \qquad k = 1, 2, ..., m, \tag{2.2}$$

where $f_k(x)$ is the original objective function and $P(x)$ is the penalty term used to penalize the solutions that violate the constraints.

2.4.2. Solving procedure. The solution procedure of the NSWOA algorithm [21, 22] is as follows: in the first stage, the set of whales and prey is randomly generated by the whale population and their position vectors are initialized. The fitness of each whale's position is then calculated according to the objective function. In the second stage, the non-dominated solutions in the initial population are determined and saved in the Pareto archive, the crowding distance of each Pareto solution is calculated, and position vectors are selected based on the crowding distance value. Next, the position vector is calculated and the positions of whales are updated using the following equations:

$$\mathbf{X}(t+1) = \mathbf{D}' * e^{bt} * \cos(2\pi l) + \mathbf{X}^*(t), \tag{2.3}$$

$$\mathbf{D}' = \left|\mathbf{X}^*(t) - \mathbf{X}(t)\right|, \tag{2.4}$$

where l is a random number $[-1, 1]$, b is a constant defining the logarithmic shape, the asterisk represents simple multiplication, and $\mathbf{D}'$ expresses the distance between the i-th whale and the prey mean best solution so far.

Note, we assume that there is a 50 % probability that a whale either follows the shrinking encircling or the logarithmic path during optimization. Mathematically, this is expressed as:

$$\mathbf{X}(t+1) = \begin{cases} \mathbf{X}^*(t) - \mathbf{X} \cdot \mathbf{X} & \text{if} \quad p < 0.5, \\ \mathbf{D}' * e^{bl} * \cos(2\pi l) + \mathbf{X}^*(t) & \text{if} \quad p > 0.5, \end{cases} \tag{2.5}$$

where p expresses a random number in the range $[0, 1]$.

The vector $\mathbf{A}$ can be used for exploration in the search for prey; specifically, vector $\mathbf{A}$ takes values greater than 1 or less than -1. Exploration follows two conditions:

$$\mathbf{D} = \left|\mathbf{C} * \mathbf{X}_{\text{rand}} - \mathbf{X}\right|, \tag{2.6}$$

$$\mathbf{X}(t+1) = \mathbf{X}_{\text{rand}} - \mathbf{A} \cdot \mathbf{D}. \tag{2.7}$$

Finally, these conditions follow: $|\mathbf{A}| > 1$ enforces exploration, enabling the WOA to find out the global optimum and avoid local optima; $|\mathbf{A}| < 1$ is used

for updating the position of the current search agent and moving toward the best solution.

In the third stage, the fitness values of all update locations of whales are calculated, new non-dominated solutions in the population are determined and saved in the Pareto files, while any dominant solutions in the Pareto files are eliminated. The crowding distance values of each Pareto solution are then calculated, and non-dominated sorting is performed according to the crowding distance mechanism. Global optimal solutions of rank 1 and rank 2 are selected, and the optimal Pareto solution set is output.

2.4.3. Entropy weight – TOPSIS comprehensive evaluation. The entropy weight method is an objective weight determination method based on the principle of information theory, which reflects the importance of each indicator by quantifying its information entropy value. The good-and-bad solution distance method (TOPSIS) is a comprehensive evaluation method widely used in multi-objective decision analysis. This method realizes the scientific evaluation and ranking of multi-index and multi-scheme systems by calculating the relative proximity of each scheme to the positive and negative ideal solutions. It is an effective method applicable to complex decision-making scenarios.

The multi-criteria decision-making approach using the entropy weight – TOPSIS method mainly includes the following implementation steps: in the initial stage, a standardized decision matrix needs to be constructed, and then the weight coefficients of each evaluation index are calculated using the entropy weight method. Based on this, the positive and negative ideal solutions of the scheme set are determined, and the Euclidean distances between each scheme and the positive and negative ideal solutions are calculated. By establishing a comprehensive evaluation function, the comprehensive score values of each scheme are calculated, and the schemes are ranked and selected based on the scores from high to low. Among them, the higher the score, the closer the scheme is to the positive ideal solution and the better the quality of the scheme. This research combines the entropy weight method with the TOPSIS method to screen out the optimal solution from the Pareto solution set optimized and generated by the NSWOA algorithm.

2.4.4. Multi-objective optimization process. The multi-objective optimization process of hobbing process parameters is as follows: the total deviation of tooth profile, the total deviation of helix, the cumulative total deviation of tooth spacing and the radial runout are determined as optimization objectives. The hob speed, the feed rate and the cutting number are determined as optimization variables, and their constraint conditions are established. The regression models of total profile deviation, total helix deviation, cumulative total deviation

of tooth spacing and radial runout based on the response surface test data are used as objective function models. These objective function models are solved by the NSWOA algorithm. The Pareto solution set of hobbing process parameters is obtained, and the optimal scheme optimized by the NSWOA algorithm is determined using the entropy weight and TOPSIS methods. The flow chart of the process is shown in Fig. 5.

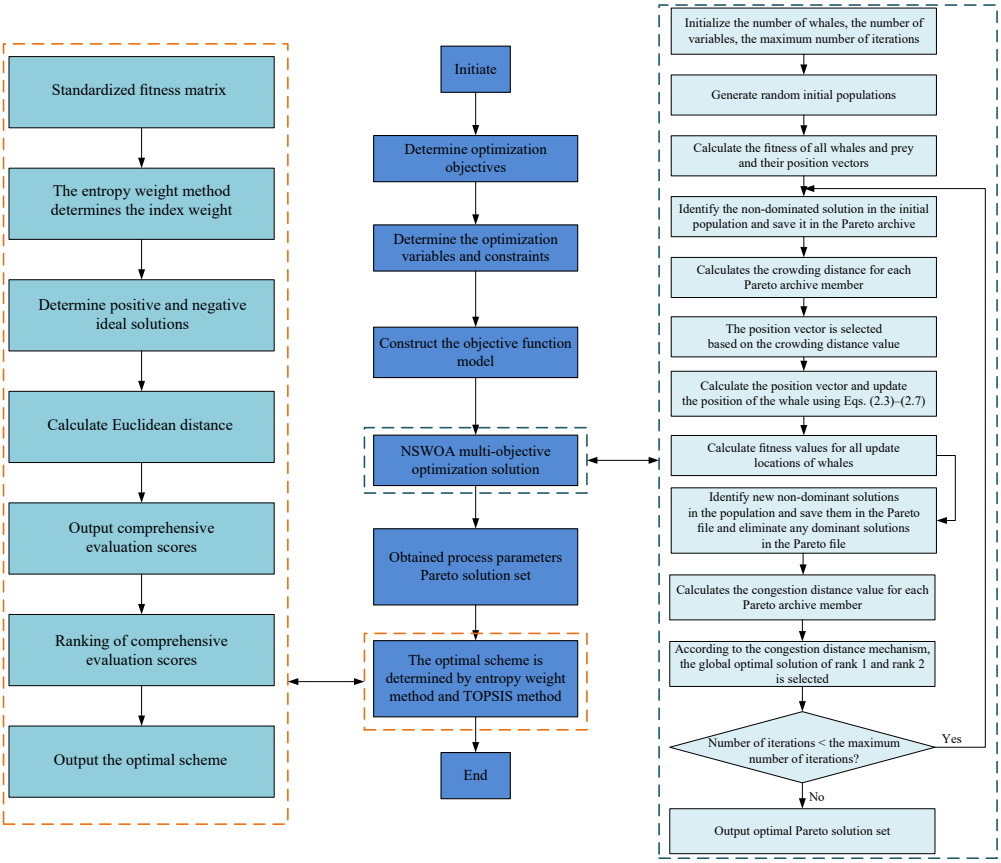

FIG. 5. Multi-objective optimization flow chart of gear hobbing process parameters.

3. RESULTS AND DISCUSSION

3.1. Establishment of mathematical model

The geometric accuracy measurement results of the response surface test are shown in Table 5. In this study, stepwise regression analysis was adopted, and Design-Expert 13.0 software was used to model the total deviation of tooth profile, the total deviation of helix, the cumulative total deviation of tooth spacing, and the radial runout. A ternary quadratic regression model of hob speed, feed rate, and back engagement with respect to the total deviation of tooth pro-

TABLE 5. Measurement results of geometric accuracy of response surface test.

No.	Total deviation of tooth profile [μm]	Total deviation of helix [μm]	Cumulative total deviation of tooth spacing [μm]	Radial runout [μm]
1	12.0	27.6	28.9	28.9
2	9.4	22.0	35.8	32.2
3	11.2	22.4	46.55	45.4
4	11.0	23.3	28.5	30.8
5	11.4	23.0	46.7	44.7
6	11.0	23.3	45.55	45.0
7	10.0	38.5	25.85	27.6
8	9.0	28.1	24.05	29.7
9	11.0	28.9	31.2	37.4
10	12.6	27.0	25.35	28.1
11	10.6	29.1	24.1	23.0
12	9.2	37.0	52.8	58.8
13	10.6	47.9	29.2	38.6
14	12.2	28.3	20.4	19.4
15	11.5	26.5	10.5	13.2
16	12.1	26.2	21.4	25.5
17	12.8	25.3	21.2	20.4

file, the total deviation of helix, the cumulative total deviation of tooth spacing and the radial runout is obtained. In order to facilitate operation and analysis in the software, the back engagement D is expressed in terms of the number of cuts D_t. The mathematical models of the tooth surface geometric accuracy established according to the response surface method (RSM) are as follows:

$$F_\alpha = 11.90472 - 0.000672V - 4.67556f + 5.20250D_t + 0.008444Vf + 0.000167VD_t + 0.8fD_t - 0.000023V^2 - 0.537778f^2 - 1.17750D_t^2, \tag{3.1}$$

$$F_\beta = 105.08944 - 0.307144V + 69.70222f - 51.335D_t - 0.005778Vf + 0.053VD_t - 6.8fD_t + 0.000125V^2 - 7.98222f^2 + 5.96D_t^2, \tag{3.2}$$

$$F_P = 236.37333 + 0.21985V - 148.10667f - 58.05333D_t + 0.002Vf + 0.034167VD_t + 5.06667fD_t - 0.000245V^2 + 25.48f^2 + 3.0075D_t^2, \tag{3.3}$$

$$F_r = 215.14611 + 0.1619V - 103.65444f - 69.37583D_t - 0.01Vf + 0.038833VD_t + 2.86667fD_t - 0.000192V^2 + 20.36444f^2 + 5.055D_t^2. \tag{3.4}$$

3.2. Model analysis

The regression analysis of these four mathematical models shows that the correlation coefficients R^2 of the total profile deviation, the total helix deviation, the cumulative total pitch deviation, and the radial runout regression models are all greater than 0.9. (According to the definition of the coefficient of correlation R^2, its value ranges from 0 to 1. When R^2 approaches 1, it indicates that the prediction accuracy of the regression model is higher, the error has less influence on the result, and the fitting effect of the model is more ideal.) This indicates that the regression models for the total profile deviation, the total helix deviation, the cumulative total pitch deviation and the radial runout have sufficient prediction accuracy.

Table 6 shows the analysis of variance (ANOVA) results of the total tooth profile deviation regression model. The F-value is the key statistic of ANOVA, used to evaluate the significant difference of variance between factors. In general, when $F \geq 4$, it indicates that the variation of design parameters has a significant impact on model performance. The P-value is used to measure the statistical significance of the F-value. If $P \leq 0.05$, it indicates that the factor has a significant impact on the response variable. In addition, when the P-value of the lack-of-fit term is greater than 0.05, it indicates that the proportion of abnormal error in the regression equation is low and that the model fits the actual data well. The F-value of the model term is 9.03 and the P-value is 0.0042, which reflects the high significance of the regression model. At the same time, the F-value

Table 6. ANOVA for regression fitting of the total deviation of tooth profile.

Source	Sum of squares	*Df*	Mean square	F-value	P-value	Significance
Model	19.33	9	2.15	9.03	0.0042	significant
V	4.65	1	4.65	19.55	0.0031	–
f	0.1250	1	0.1250	0.5254	0.4921	–
D_t	1.53	1	1.53	6.44	0.0388	–
Vf	3.61	1	3.61	15.17	0.0059	–
VD_t	0.0025	1	0.0025	0.0105	0.9212	–
fD_t	1.44	1	1.44	6.05	0.0435	–
V^2	1.17	1	1.17	4.92	0.0620	–
f^2	0.3853	1	0.3853	1.62	0.2438	–
D_t^2	5.84	1	5.84	24.54	0.0016	–
Residual	1.67	7	0.2379	–	–	–
Lack-of-fit	0.2575	3	0.0858	0.2438	0.8621	not significant
Pure error	1.41	4	0.3520	–	–	–
Cor total	21.00	16	–	–	–	–
$R^2 = 0.9207$						

of the lack-of-fit term is 0.2438 and the P-value is 0.8621, which further indicates that the influence of the lack-of-fit is not significant compared with the pure error, and the model has strong explanatory ability and reliability. In this case, V, D_t, Vf, fD_t, and D_t^2 are important factors. The correlation coefficient R^2 of the model is 0.9207, indicating that the model has a high degree of fit.

According to the ANOVA results of the total helix deviation regression model shown in Table 7, the F-value of the model term is 33.7, and the P-value is less than 0.0001, indicating that the regression model has extremely high significance. In addition, the F-value of the lack-of-fit term is 0.1393 and the P-value is 0.9314, indicating that the influence of the lack-of-fit is not significant compared with the pure error. The model can fully explain the variation in the data, and has good applicability and reliability. In this case, V, f, D_t, VD_t, fD_t, V^2, f^2, and D_t^2 are significant factors. The correlation coefficient R^2 of the model is 0.9774, and the degree-of-fit is very high.

Table 7. ANOVA for regression fitting of the total helix deviation.

Source	Sum of squares	*Df*	Mean square	*F*-value	*P*-value	Significance
Model	719.11	9	79.90	33.70	<0.0001	significant
V	36.12	1	36.12	15.24	0.0059	–
f	16.82	1	16.82	7.09	0.0323	–
D_t	49.00	1	49.00	20.67	0.0026	–
Vf	1.69	1	1.69	0.7127	0.4264	–
VD_t	252.81	1	252.81	106.62	<0.0001	–
fD	104.04	1	104.04	43.88	0.0003	–
V^2	33.25	1	33.25	14.02	0.0072	–
f^2	84.88	1	84.88	35.80	0.0006	–
D_t^2	149.56	1	149.56	63.08	<0.0001	–
Residual	16.60	7	2.37	–	–	–
Lack-of-fit	1.57	3	0.5233	0.1393	0.9314	not significant
Pure error	15.03	4	3.76	–	–	–
Cor total	735.71	16	–	–	–	–
$R^2 = 0.9774$						

Table 8 shows the ANOVA results of the regression model of cumulative total deviation of tooth spacing. The F-value of the model term is 11.18 and the P-value is 0.0022, indicating that the regression equation is highly significant. At the same time, the F-value of the lack-of-fit term is 1.59 and the P-value is 0.3235, indicating that the influence of the lack-of-fit is not significant compared with the pure error, and the model can effectively explain the trends in data variation, and has strong reliability and applicability. In this case, V, f, D_t,

Table 8. ANOVA for regression fitting of the cumulative total deviation of tooth spacing.

Source	Sum of squares	*Df*	Mean square	*F*-value	*P*-value	Significance
Model	1947.25	9	216.36	11.18	0.0022	significant
V	203.01	1	203.01	10.49	0.0143	–
f	320.04	1	320.04	16.54	0.0048	–
D_t	248.64	1	248.64	12.85	0.0089	–
Vf	0.2025	1	0.2025	0.0105	0.9214	–
VD_t	105.06	1	105.06	5.43	0.0526	–
fD_t	57.76	1	57.76	2.99	0.1276	–
V^2	128.18	1	128.18	6.63	0.0368	–
f^2	864.93	1	864.93	44.71	0.0003	–
D_t^2	38.08	1	38.08	1.97	0.2034	–
Residual	135.42	7	19.35	–	–	–
Lack-of-fit	73.76	3	24.59	1.59	0.3235	not significant
Pure error	61.66	4	15.42	–	–	–
Cor total	2082.67	16	–	–	–	–
$R^2 = 0.9350$						

V^2, and f^2 are significant factors. The correlation coefficient of the model is 0.9350, and the degree-of-fit is high.

According to the ANOVA results for the radial runout regression model presented in Table 9, the F-value of the model term is 13.6 and the P-value

Table 9. ANOVA for the radial runout regression fitting.

Source	Sum of squares	*Df*	Mean square	*F*-value	*P*-value	Significance
Model	2005.73	9	222.86	13.6	0.0012	significant
V	75.65	1	75.65	4.61	0.0688	–
f	539.56	1	539.56	32.92	0.0007	–
D_t	494.55	1	494.55	30.17	0.0009	–
Vf	5.06	1	5.06	0.3088	0.5957	–
VD_t	135.72	1	135.72	8.28	0.0237	–
fD_t	18.49	1	18.49	1.13	0.3235	–
V^2	78.58	1	78.58	4.79	0.0647	–
$f2$	552.49	1	552.49	33.7	0.0007	–
D_t^2	107.59	1	107.59	6.56	0.0374	–
Residual	114.74	7	16.39	–	–	–
Lack-of-fit	36.53	3	12.18	0.6228	0.6367	Not significant
Pure error	78.21	4	19.55	–	–	–
Cor total	2120.47	16	–	–	–	–
$R^2 = 0.9459$						

is 0.0012, indicating that the regression equation is highly significant. In addition, the F-value of the lack-of-fit term is 0.6228 and the P-value is 0.6367, indicating that the influence of the lack-of-fit is not significant compared with the pure error, and the model can fully explain the variation in the data, and has good applicability and reliability. In this case, f, D_t, VD_t, f^2, and D_t^2 are significant factors. The correlation coefficient of the model is 0.9459, and the degree-of-fit is high.

3.3. Response surface diagram analysis

The response surface diagram can be used to more intuitively understand the interaction effects between factors, the variation trends of response variables, and the direction and intensity of interactions. Figure 6 shows the response surface diagrams for the total tooth profile deviation, in which Fig. 6a presents the response surface diagrams of the influence of hob speed and feed rate on the total tooth profile deviation. When the feed rate is constant, the total deviation

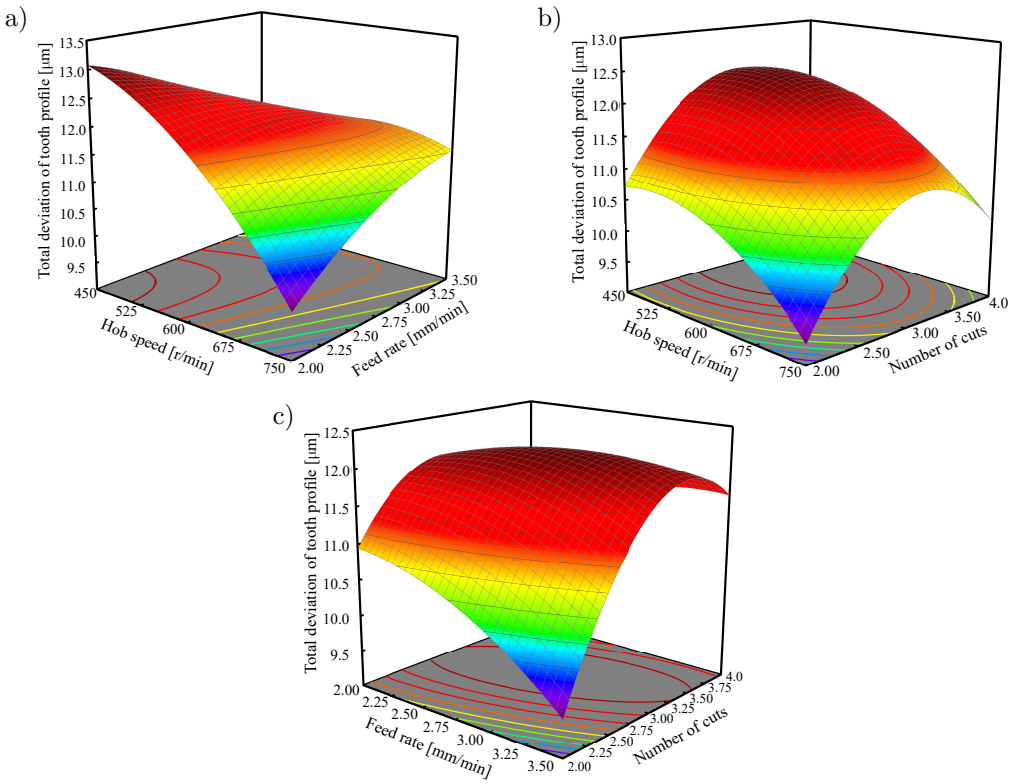

FIG. 6. Response surface diagrams of the total tooth profile deviation F_α: a) response surface influenced by V and f for F_α; b) response surface influenced by V and D_t for F_α; c) response surface influenced by f and D_t for F_α.

of the tooth profile decreases as the hob speed increases. When the hob speed is constant, the total deviation of the tooth profile decreases slowly as the fed rate increases. The increase of hob speed and feed rate can reduce the total profile deviation, but the influence of hob speed on the total profile deviation is greater. Figure 6b shows the response surface diagram of the influence of the hob rotation speed and the cut number on the total tooth profile deviation. It can be seen that the influence of hob speed and number of cuts on the total tooth profile deviation is very significant. When the number of cuts is small, the total deviation of tooth profile decreases with increasing hob speed. With the increase cut number, the total deviation of tooth profile increases significantly, which also indicates that the increase of the number of cuts has a great effect on the total tooth profile deviation. When the hob speed is high, it can partially offset the influence of the number of cuts on the total deviation of tooth profile; Fig. 6c depicts the response surface diagram of the influence of feed rate and number of cuts on the total profile deviation. When the number of cuts is small, the total profile deviation decreases with increasing feed rate. When the number of

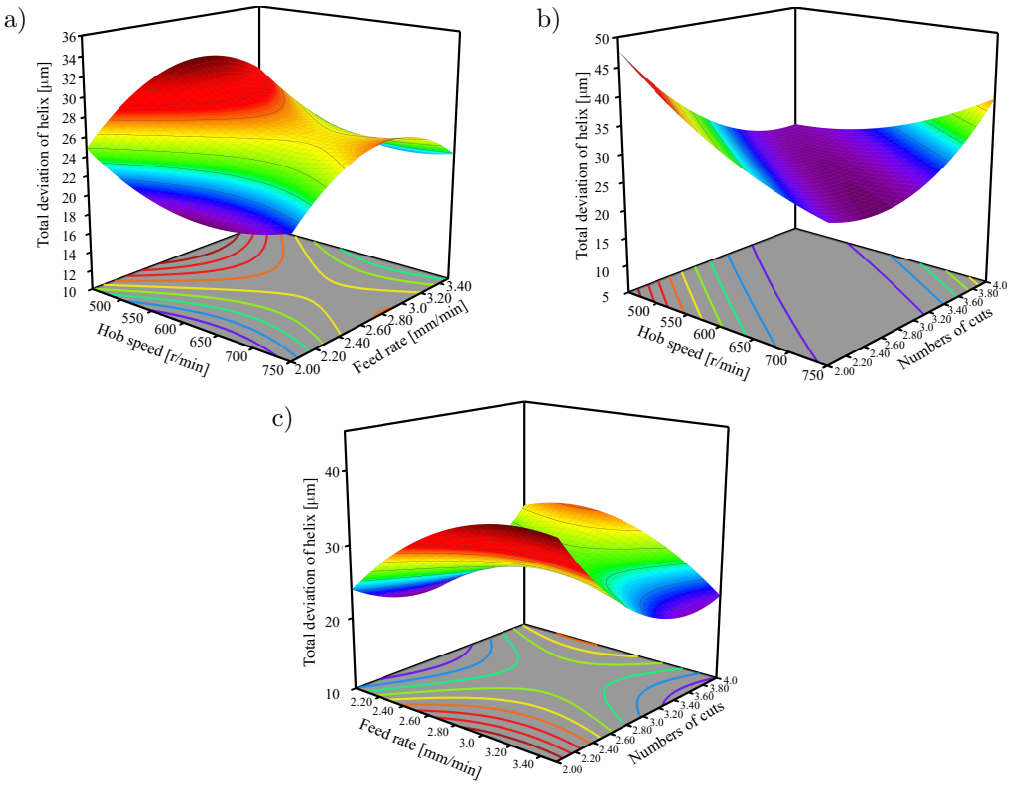

FIG. 7. Response surface diagram for the total helix deviation F_β: a) response surface influenced by V and f for F_β; b) response surface influenced by V and D_t for F_β; c) response surface influenced by f and D_t for F_β.

cuts increases, the total deviation of tooth profile also increases significantly, especially at 3 cuts, where the impact on the total deviation of tooth profile is most significant.

Figure 7 shows the response surface diagrams for the total helix deviation, and Fig. 7a presents the response surface diagram of the combined influence of the hob speed and the feed rate on the total helix deviation. When the feed rate is constant, the total helix deviation decreases as the hob speed increases. When the hob speed is constant, the total helix deviation increases slowly as the feed rate increases. Figure 7b shows the response surface diagram of the influence of the hob speed and the number of cuts on the total helix deviation. It can be seen that the influence of the hob speed and the number of cuts on the total helix deviation is very significant; when the number of cuts is small, the total helix deviation decreases as the hob speed increases. When the number of cuts is large, the total helix deviation increases as the hob speed increases, which indicates that the increase of the number of cuts has a great effect on the total helix deviation. Figure 7c shows the response surface diagram of the influence of the feed rate and the number of cuts on the total helix deviation. When the number of cuts is small, the total helix deviation increases as the feed rate increases. When the number of cuts increases, the total helix deviation decreases significantly, especially at 3 cuts, where the influence on the total helix deviation is most significant.

Figure 8 depicts the response surface diagrams for the cumulative total deviation of tooth spacing, where Fig. 8a is the response surface diagram for the combined influence of the hob speed and the feed rate on the cumulative total deviation of tooth spacing. When the feed rate is constant, the cumulative total deviation of tooth spacing increases as the hob speed increases. When the hob speed is constant, the cumulative total deviation of tooth spacing increases rapidly with increasing feed rate. Figure 8b shows the response surface diagram of the influence of the hob speed and the number of cuts on the cumulative total deviation of tooth spacing. When the number of cuts is fixed, the cumulative total deviation of tooth spacing increases with increasing hob speed; with the increase of the number of cuts, the cumulative total deviation of tooth spacing shows no significant change, which indicates that this increase has little effect on the cumulative total deviation of tooth spacing. Figure 8c presents the response surface diagram of the influence of the feed rate and the number of cuts on the cumulative total deviation of tooth spacing. When the number of cuts is constant, the cumulative total deviation of tooth spacing first decreases and then increases with the increase of feed rate; with the increase of the number of cuts, the cumulative total deviation of tooth spacing decreases slowly.

Figure 9 shows the response surface diagrams of radial runout, where Fig. 9a displays the response surface diagram of the influence of the hob speed and the

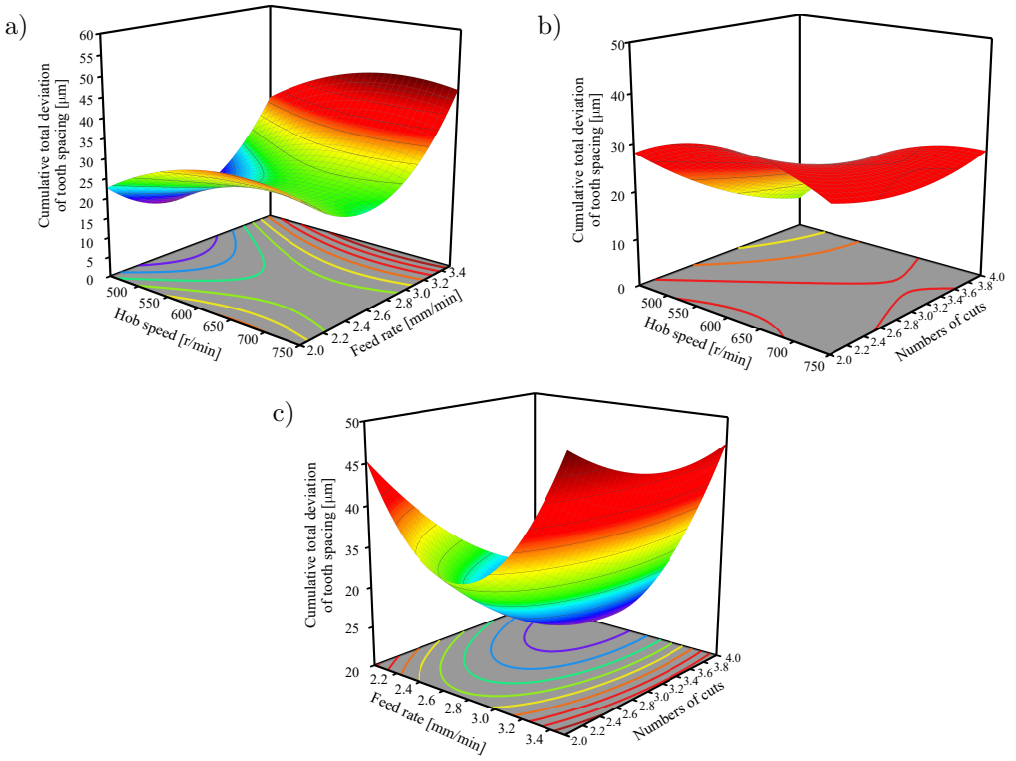

FIG. 8. Response surface diagram of the cumulative total deviation of tooth spacing F_p: a) response surface influenced by V and f for F_p; b) response surface influenced by V and D_t for F_p; c) response surface influenced by f and D_t for F_p.

feed rate on radial runout. When the feed rate is constant, the radial runout increases with the increase of hob speed. When the hob speed is constant, the radial runout increases rapidly with the increase of feed rate. Figure 9b presents the response surface diagram of the influence of the hob speed and the number of cuts on radial runout. When the number of cuts is small, the radial runout first increases and then decreases with the increase of hob speed. When the number of cuts increases, the radial runout decreases slowly. Figure 9c shows the response surface diagram of the influence of the feed rate and the number of cuts on the radial runout. When the number of cuts is constant, the radial runout first decreases and then increases with the increase of feed rate. When the number of cuts increases, the radial runout decreases slowly.

3.4. Optimization results and analysis

The optimization parameters of the NSWOA algorithm are set as follows: the initial population is 100, and the number of iterations is 500. The Pareto

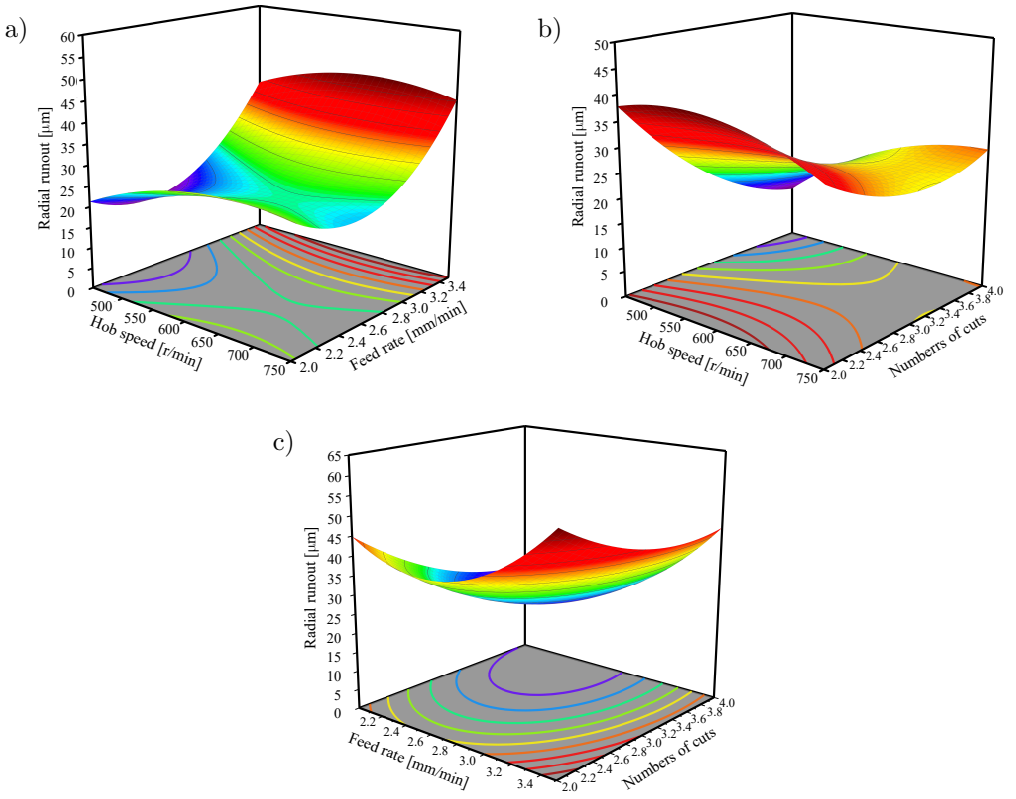

FIG. 9. Response surface diagram of the radial runout F_r: a) response surface influenced by V and f for F_r; b) response surface influenced by V and D_t for F_r; c) response surface influenced by f and D_t for F_r.

optimal solution set was obtained through the NSWOA algorithm optimization, and the results of the Pareto optimal solution set are shown in Fig. 10. The figure shows that the optimal combination of gear hobbing process parameters ensures that all data points satisfy the requirements for the machining and geometric accuracy. Analysis indicates that there is a significant negative correlation between the total deviation of tooth profile and the total helix deviation, the cumulative total deviation of pitch, and radial runout. The specific observations are as follows: with the increase of the total deviation of the tooth profile, the total helix deviation, the cumulative total pitch deviation, and the radial runout show a decreasing trend. Meanwhile, there is a significant positive correlation between the total helix deviation, the cumulative total pitch deviation, and radial runout. That is, as the total helix deviation increases, the cumulative total pitch deviation and the radial runout also increase accordingly. In addition, there is also a significant positive correlation between the cumulative total pitch deviation and the radial runout.

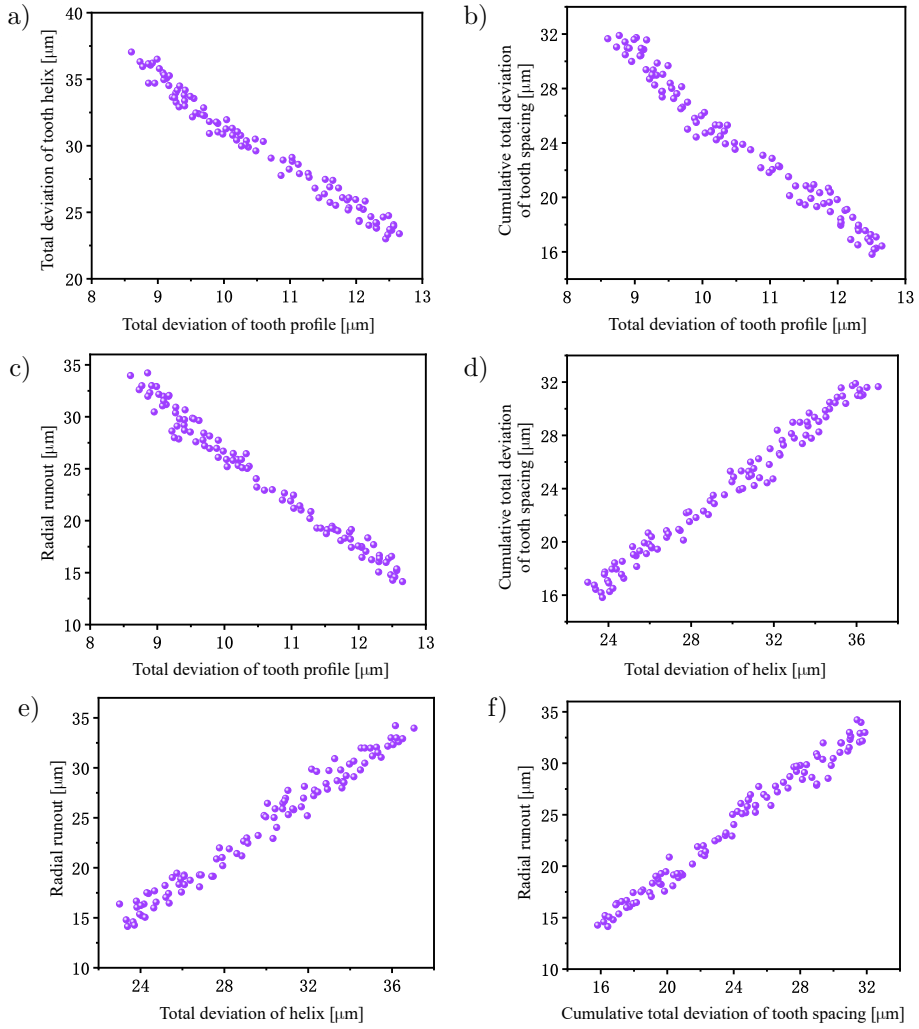

FIG. 10. Pareto optimal solution set for optimization of hobbing process parameters.

In this paper, the entropy weight-TOPSIS comprehensive evaluation method was used to conduct a systematic analysis of the Pareto solution set optimized and generated by the NSWOA algorithm. First, the original data were standardized, and the weight vectors of each index were calculated using the entropy weight method as $[0.26971, 0.22237, 0.27536, 0.23256]^{\mathrm{T}}$. Subsequently, through weighted standardization processing, the positive ideal solution was determined as [1, 1, 1, 1], and the negative ideal solution as [0, 0, 0, 0]. Based on this, the Euclidean distances between each Pareto solution and the positive and negative ideal solutions were calculated, and the comprehensive score value was obtained. The final evaluation results are shown in Table 10.

Table 10. Entropy weight method – TOPSIS comprehensive evaluation.

Scheme sequence number	Positive ideal solution distance (D+)	Negative ideal distance (D−)	Composite score index	Rank
1	0.8464	0.5194	0.3803	91
2	0.4529	0.6204	0.5780	34
3	0.5315	0.4851	0.4772	58
4	0.4480	0.7106	0.6134	16
5	0.7003	0.4624	0.3977	83
...	...	...	...	...
96	0.4524	0.6313	0.5826	32
97	0.5013	0.8401	0.6263	3
98	0.6005	0.4769	0.4427	67
99	0.5001	0.5060	0.5029	48
100	0.5500	0.4794	0.4657	61

In traditional production practice, gear hobbing processing usually adopts the average value of process parameter design: specifically, the hob speed is 600 r/min, the feed rate is 2.75 mm/min, and the depth of cut is 1.125 mm. After optimization, the process parameters were adjusted to a hob speed of 750 r/min, a feed rate of 2 mm/min, and a back engagement of 1.6875 mm. According to the comparative analysis of geometric accuracy before and after optimization presented in Table 11, the optimized scheme significantly improved the geometric accuracy of gear processing. Among them, the total deviation of the tooth profile decreased by 8.04 %, the total helix deviation decreased by 9.17 %, the cumulative total pitch deviation decreased by 3.88 %, and the radial runout decreased by 7.45 %. The test results show that the optimized process parameters can effectively improve the geometric accuracy of gear hobbing processing, providing a solution for achieving high-precision manufacturing of gears.

Table 11. Comparison of schemes.

	Total deviation of tooth profile [μm]	Total deviation of helix [μm]	Cumulative total deviation of tooth spacing [μm]	Radial runout [μm]
Experience scheme	12.1	26.2	21.4	25.5
Optimized scheme	11.2	24	20.6	23.6

3.5. Algorithm performance comparison

In this paper, the second-generation non-dominated sorting genetic algorithm (NSGA-II) and the NSWOA algorithm are selected for performance comparison and analysis. The algorithm parameters are uniformly set as: population

size: 100, and iteration times: 500. In the implementation of the NSGA-II algorithm, the interval selection strategy is adopted for chromosome screening, and a genetic operation strategy of two-point crossover and point mutation is adopted. Among them, the crossover probability is set to 0.9, and the mutation probability is set to 0.1. Figure 11 shows the distribution of the Pareto solution set obtained from a single run of the NSGA-II algorithm.

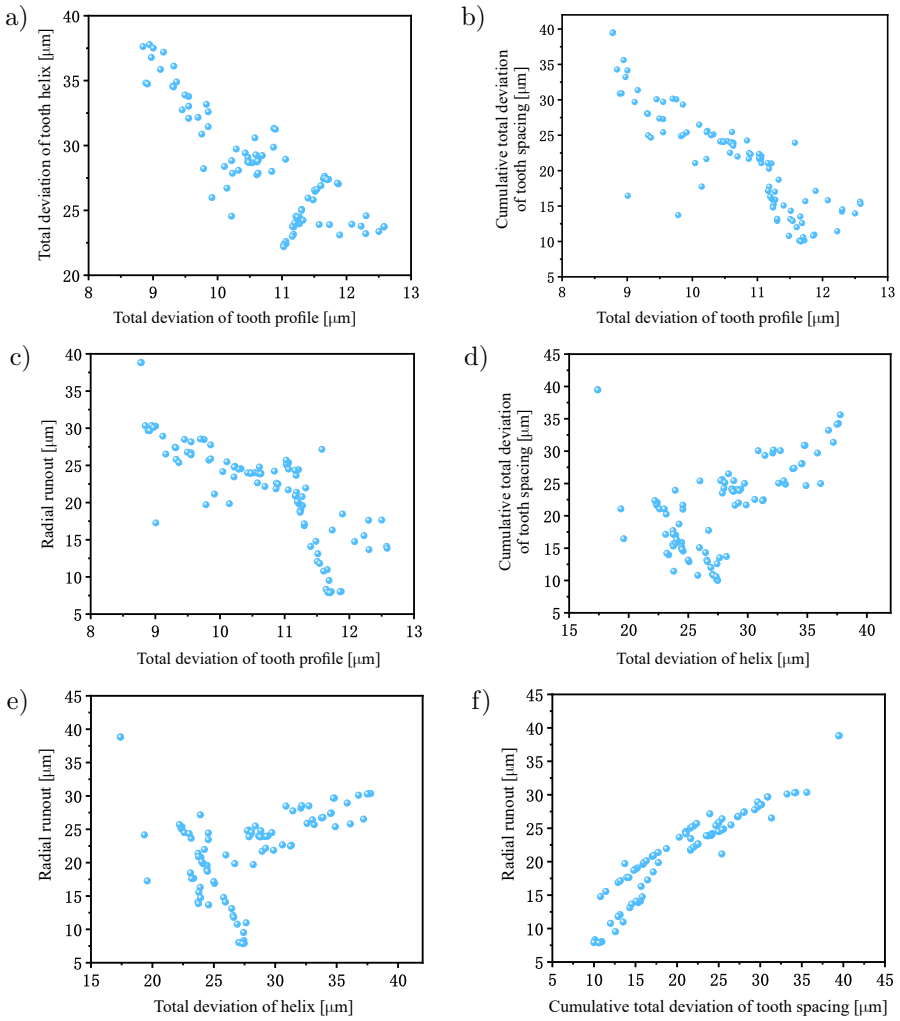

FIG. 11. Non-dominated solution diagrams of NSGA-II algorithm.

Through multiple independent tests of the two algorithms, Table 12 presents the statistical performance comparison data for 10 runs each of NSGA-II and NSWOA. It can be seen from the data analysis in Table 12 that NSGA-II has obvious advantages in computational efficiency, and its running time is less

Table 12. Comparison of algorithm performance and running time.

Algorithm	Parameter	Total deviation of tooth profile [μm]	Total deviation of helix [μm]	Cumulative total deviation of tooth spacing [μm]	Radial runout [μm]	Running time [s]
NSGA-II	Optimal value	8.5	17.25	9.98	8.2	2.8
	Mean value	12.36	26.0	10.33	23.0	3.2
NSWOA	Optimal value	8.45	17.0	8.0	7.63	9.39
	Mean value	10.43	24.5	9.5	20.6	9.48

than 50 % of that of NSWOA. However, NSWOA performs more prominently in the optimization performance of the objective functions. Both its optimal solution quality and average solution quality are superior to those of NSGA-II, demonstrating a stronger global search capability. The comprehensive comparison shows that in the current application scenario, the NSWOA shows higher applicability and can approach the optimal solution of the problem more effectively compared with NSGA-II.

4. Conclusions

In this paper, the RSM was used to study the process of gear hobbing. The results of the hobbing experiments, model building, and optimization analysis show that:

1. Based on the response surface test data, regression models for the total profile deviation, the total helix deviation, the cumulative total deviation of tooth spacing, and the radial runout were established, and the reliability of these models was tested by ANOVA.
2. The interaction effects of different process parameters on the total profile deviation, the total helix deviation, the cumulative total deviation of tooth spacing, and the radial runout were analyzed using response surface diagrams. The interactions of the hob speed, the feed rate, and the number of cuts on these responses were significant. Among them, the hob rotational speed had the greatest influence on the geometric accuracy, followed by the feed rate. The number of cuts had a relatively large influence on the total tooth profile deviation and the total helix deviation, but a relatively small influence on the cumulative total deviation of the tooth spacing and the radial runout.
3. Objective functions for the total profile deviation, the total helix deviation, the cumulative total deviation of tooth spacing and the radial runout were established respectively. With the hob speed, the feed rate and the cut

number as optimization variables, and the total profile deviation, the total helix deviation, the cumulative total deviation of tooth spacing, and the radial runout as optimization objectives, the established model was solved using the NSWOA algorithm. A Pareto solution set within the constraint range was obtained, and the optimal scheme optimized by the NSWOA algorithm was determined by combining the entropy weight and TOPSIS methods. Compared with the empirical scheme, after optimization, the total profile deviation was reduced by 8.04 %, the total helix deviation was reduced by 9.17 %, the cumulative total deviation of tooth spacing by 3.88 %, and the radial runout by 7.45 %.

Fundings

This research was supported by the Natural Science Foundation of Gansu Province (25JRRA092) and the College Teachers Innovation Fund of Gansu Province (2025A-029).

Conflict of interests

The authors declare that they have no known competing financial interests or personal relationships that could have appeared to influence the work reported in this paper.

Authors' contributions

Yazhou Wang performed editing and reviewing of the paper, obtained funding, conceptualized the original paper, conducted resource management and formal analysis. Xiaohui Yin conceptualized the study, wrote the original draft, performed the analysis and contributed to data interpretation, conducted specific research using relevant software and methodologies, investigations, visualizations, carried out formal analyses.

All authors reviewed and approved the final manuscript.

References

1. Chen Y., Liu X., Yan X., Yang Y., Investigation on geometrical morphology of tooth surface finished by green high-speed dry hobbing for gear precision machining, *International Journal of Precision Engineering and Manufacturing-Green Technology*, **10**(5): 1141–1154, 2023, https://doi.org/10.1007/s40684-022-00459-3.

2. Sun S.L., Wang S.L., Wang Y., Lim T.C., Yang Y., Prediction and optimization of hobbing gear geometric deviations, *Mechanism and Machine Theory*, **120**: 288–301, 2018, https://doi.org/10.1016/j.mechmachtheory.2017.09.002.

3. Hu Q.S., Li H., Research on hobbing accuracy of flexspline tooth profile of harmonic drive, *Journal of Advanced Mechanical Design Systems and Manufacturing*, **18**(2), 2024, https://doi.org/10.1299/jamdsm.2024jamdsm0008.

4. Wang J., Wang J., Dong J.P., Prediction and optimization of hobbing parameters for minimizing energy consumption and gear geometric deviations, *Advances in Mechanical Engineering*, **16**(4), 2024, https://doi.org/10.1177/16878132241236374.

5. Matsuo K., Suzuki Y., Fujiki K., Analysis of the effect on gear accuracy of workpiece/tool positioning accuracy in the hobbing process, *Journal of Advanced Mechanical Design Systems and Manufacturing*, **11**(6), 2017, https://doi.org/10.1299/jamdsm.2017jamdsm0071.

6. Zhou J.L., Sun Z.H., Tan Q., Xie Y.C., Dry gear hobbing machining experiment and research on process parameters, *Applied Mechanics and Materials*, **538**: 95–99, 2014, https://doi.org/10.4028/www.scientific.net/AMM.538.95.

7. Dong X., Liao C., Shin Y.C, Zhang H.H., Machinability improvement of gear hobbing viaprocess simulation and tool wear predictions, *The International Journal of Advanced Manufacturing Technology*, **86**: 2771–2779, 2016, https://doi.org/10.1007/s00170-016-8400-3.

8. Klocke F., Brecher C., Löpenhaus C., Krömer M., Calculating the workpiece quality using a hobbing simulation, *Procedia CIRP*, **41**: 687–691, 2016, https://doi.org/10.1016/j.procir.2015.12.045.

9. Huai W.B., Shi Y.Y., Du Y.Y., Dong X., Optimization of milling process parameters for multi-objective superalloy GH4169 [in Chinese], *Modern Manufacturing Engineering*, **2020**(11), 2020, https://doi.org/10.16731/j.cnki.1671-3133.2020.11.001.

10. Kane M.M., Ivanov B.V., Zagorskaya N.B., Optimizing the hobbing of cylindrical gears, *Russian Engineering Research*, **34**: 526–529, 2014, https://doi.org/10.3103/S1068798X14080061.

11. Li X., Yang Y., Zou Z., Deng F., Wang L., Tang Q., Study on the effect of force-thermal coupling error on the gear hobbing accuracy and its visualization, *The International Journal of Advanced Manufacturing Technology*, **102**(1): 583–594, 2019, https://doi.org/10.1007/s00170-018-3186-0.

12. Sant'Anna D.R., Mundim R.B., Borille A.V., Gomes J.O., Experimental approach for analysis of vibration sources in a gear hobbing machining process, *Journal of the Brazilian Society of Mechanical Sciences and Engineering*, **38**(3): 789–797, 2016, https://doi.org/10.1007/s40430-014-0300-6.

13. Biswas A., Kalayci C.B., Mirjalili S. [Eds], *Advances in Swarm Intelligence: Variations and Adaptations for Optimization Problems, Studies in Computational Intelligence*, Springer Cham, 2023, https://doi.org/10.1007/978-3-031-09835-2.

14. Wu X.Q., Zhang C.Y., Optimization algorithm of hobbing cutting parameters based on particle swarm optimization SVR, [in:] *2018 International Conference on Computational Science and Engineering*, pp. 12–17, 2018.

15. Wang Y.Z., Xu H.K., Shen H., Wang G., Wang Z., A study on the effect of gear hobbing process parameters on the residual stress of the tooth root, *Applied Sciences*, **14**(2): 597, 2024, https://doi.org/10.3390/app14020597.

16. Yuan B., Han J., Wu L.L., Tian X., Xia L., Comprehensive contour error prediction model and experimental study of hobbing tooth surface based on particle swarm optimization [in Chinese], *China Mechanical Engineering*, **27**(20): 2705–2711, 2016, https://doi.org/10.3969/j.issn.1004-132X.2016.20.002.

17. International Organization for Standardization, *Cylindrical gears – ISO system of flank tolerance classification. Part 1: Definitions and allowable values of deviations relevant to flanks of gear teeth* (ISO Standard No. 1328-1:2013), 2013, https://www.iso.org/standard/45309.html.

18. Sanjeevi R., Kumar G.A., Krishanan B.R., Optimization of machining parameters in plane surface grinding process by response surface methodology, *Materials Today: Proceedings*, **37**(Part 2): 85–87, 2021, https://doi.org/10.1016/j.matpr.2020.04.075.

19. Wang Y., Wang G., Fan Y., Zhang H., Liu Y., A virtual measurement method for evaluating the gear radial composite deviation based on point cloud data, *Results in Engineering*, **22**: 102380, 2024, https://doi.org/10.1016/j.rineng.2024.102380.

20. Kharka V., Jain N.K., Gupta K., Influence of MQL and hobbing parameters on microgeometry deviations and flank roughness of spur gears manufactured by MQL assisted hobbing, *Journal of Materials Research and Technology*, **9**(5): 9646–9656, 2020, https://doi.org/10.1016/j.jmrt.2020.06.085.

21. Jangir P., Jangir N., Non-dominated sorting whale optimization algorithm (NSWOA): A multi-objective optimization algorithm for solving engineering design problems, *Global Journal of Researches in Engineering*, **17**(F4): 15–42, 2017, retrieved from https://engineeringresearch.org/index.php/GJRE/article/view/1643.

22. Mirjalili S., Dong J.S., Lewis A. [Eds], *Nature-Inspired Optimizers. Theories, Literature Reviews and Applications*, Springer Cham, 2020, https://doi.org/10.1007/978-3-030-12127-3.

Received October 23, 2024; revised May 14, 2025; accepted June 8, 2025; published pre-proof December 12, 2025; published online January 13, 2026.